Model Predictive Control of a Single-Phase Five-Level VIENNA Rectifier

Vitor Monteiro
Centro ALGORITMI
University of Minho
Guimaraes, Portugal
vmonteiro@dei.uminho.pt

Catia Oliveira
Centro ALGORITMI
University of Minho
Guimaraes, Portugal
c.oliveira@dei.uminho.pt

Tiago Sousa
Centro ALGORITMI
University of Minho
Guimaraes, Portugal
tsousa@dei.uminho.pt

Joao L. Afonso
Centro ALGORITMI
University of Minho
Guimaraes, Portugal
jla@dei.uminho.pt

***Abstract*—Power converters and control strategies are very vital for the increasing sustainability of the power grid targeting smart grids. In these circumstances, it is proposed a novel single-phase five-level (SP5L) VIENNA rectifier digitally controlled by a model predictive control (MPC) with fixed switching frequency, which can be useful for a variety of applications with a robust current tracking. The proposed SP5L VIENNA rectifier is an advancement of the classical three-level VIENNA rectifier, also contributing to preserve power quality, and exhibiting the advantage of operating with more voltage levels at the expense of few additional switching devices. The proposed topology is introduced and correlated with the classical solutions of active rectifiers. The operation principle is introduced and used to describe the MPC, which is given in detail, as well as the necessary modulation strategy. The results were obtained for a set of various operating conditions, both in terms of reference of current and grid-side voltage, as well as in steady-state and transient-state, proving the benefits of the proposed SP5L VIENNA rectifier and the accurate and precise use of the MPC to control the grid-side current.**

Keywords—Model Predictive Control, Five-Level VIENNA Rectifier, Active Rectifier, Smart Grid, Power Quality.

I. INTRODUCTION

The notoriety of active rectifiers is well explicit based on the several topologies introduced along the last few decades. Such notoriety is due to the contribution to improve power quality issues, operating with high power factor and controlled current [1][2][3]. The active rectifier has a similar behavior as a linear load operating with unitary power factor with the added value of permitting to operate with sinusoidal currents even when supplied with a distorted voltage. Depending on the characteristics of the final application, numerous topologies can be noticed in the literature, each one exhibiting varied stages of the complication of power electronics arrangement and digital controllability [4] A concentrated presentation of the fundamental active rectifiers is presented in [5], where are highlighted the principle of operation and the foremost distinctive aspects of each one. Active rectifiers are also well identified in the literature as power-factor-correction (PFC) topologies, where, besides operating with unitary power factor, most PFC topologies also function with sinusoidal current [6]. Examining more in detail the distinct topologies, the classification regarding the multilevel property is an important characteristic, assuming an ever-greater preponderance due to the emerging technologies of power electronics. Succinctly, the multilevel consents to reduce the voltage stress affected to the power devices and reduce the constraints of connecting passive filters.

Examining in an industrial perspective, the more commonplace multilevel rectifiers are based on NPC, cascade, and Vienna-type [7][8]. Particularly analyzing the VIENNA rectifier, it was originally planned for three-phase systems, employing three switching devices. In [9] and [10] are presented three-phase single-stage rectifiers. In [11] is presented an evaluation regarding active rectifiers for EV chargers considering the efficiency perspective. Particularly regarding the VIENNA rectifier, it is the focus of the application of dedicated control theories and modulations as demonstrate in [12], [13], [14], and [15]. Beside power converters, regarding control, predictive strategies with different approaches are gaining each more preponderance for several applications within power electronics, as investigated in [16], [17], and [18].

The single-phase five-level (SP5L) VIENNA rectifier is exhibited in Fig. 1, which was originally presented and experimentally validated in [19]. The SP5L VIENNA rectifier can be used for a large variety of applications in future smart grids, such as electric mobility in battery chargers and active rectifiers for smart controllable electrical appliances for ensuring high-levels of power quality. It aggregates specific essential benefits in terms of operation with five-levels, operation without the double-boost feature, and reduced quantity of power devices. This topology holds a split dc-link with the central point attached to the neutral wire and using a bidirectional cell (two devices in common-emitter). The whole information of the SP5L VIENNA rectifier is conferred in section II, where it is introduced its principle of operation. In the scope of this paper, the grid-side current of the SP5L VIENNA rectifier is controlled with a model-predictive-control (MPC) strategy, where the main differencing focus is the operation with a fixed switching frequency, carrying a set of important advantages when confronted with the classical MPC based on a variable switching frequency. The mathematical formulation of the MPC, based on continuous-control-set, applied to the SP5L VIENNA rectifier is introduced in section III, and the validation both in steady-state and transient-state is established in section IV, while the main remarkable aspects are summarized in section V.

II. SINGLE-PHASE FIVE-LEVEL VIENNA RECTIFIER: EXPLANATION OF THE PRINCIPLE OF OPERATION

As demonstrated in Fig. 1, the SP5L VIENNA rectifier is composed by six diodes, by a switching device, and by a bipolar and bidirectional cell (which can be formed by different arrangements, where one of the main is presented in Fig. 1). In the scope of this paper, it was considered the most convenient arrangement that is based on a common-emitter configuration (in terms of practical implementation, this arrangement has an important added value because there is a common point: the emitters). Moreover, it is considered that these two switching devices are not controlled individually,

978-1-7281-7660-4/21/$31.00 ©2021 IEEE

therefore, from the control point of view, the bipolar and bidirectional cell is seen as a single switching device (S_b).

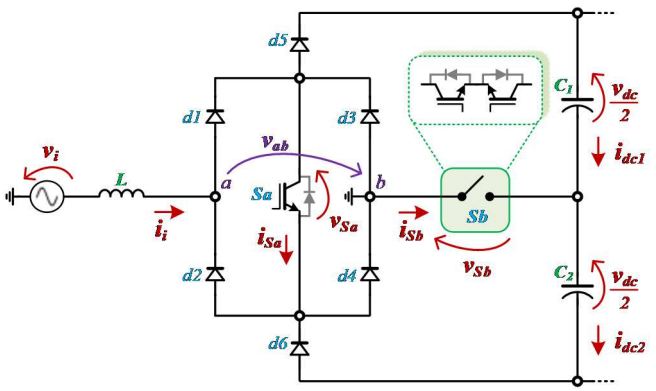

Fig. 1. Topology of the single-phase five-level (SP5L) VIENNA rectifier.

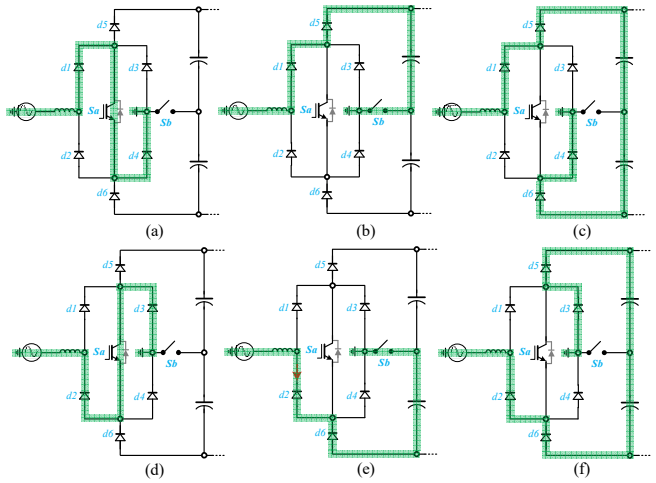

Fig. 2. Valid states of the single-phase five-level (SP5L) VIENNA rectifier to define the principle of operation in both positive ((a) to (c)) and negative ((d) to (f)) half-cycles.

The valid states of the SP5L VIENNA rectifier are presented in Fig. 2. As shown, obviously, with the objective of obtaining the five-levels, two states are defined for the positive half-cycle, also two states for the negative half-cycle and the zero state, which can be defined equally for both half-cycles or, aiming to distribute the power losses among the diodes and switching devices, two states can be defined for obtaining the zero level. Throughout the positive half-cycle, when the switching device *Sa* is on and the switching device *Sb* is off, the SP5L VIENNA rectifier is forced to operate with the zero-voltage level. In this case, the voltage v_{ab} is 0 V. On the other hand, also throughout the positive half-cycle, when the switching device *Sa* is off and the switching device *Sb* is on, the SP5L VIENNA rectifier is forced to operate with the voltage level $+v_{dc}/2$. In this case, the voltage v_{ab} is $+v_{dc}/2$. When the switching device *Sa* is off and the switching device *Sb* is also off, the SP5L VIENNA rectifier is forced to operate with the voltage level $+v_{dc}$. In this case, the voltage v_{ab} is $+v_{dc}$. Depending on the voltage level, the inductance stores or delivers energy to the circuit. On the opposite side, throughout the negative half-cycle, when the switching device *Sa* is on and the switching device *Sb* is off, the SP5L VIENNA rectifier is forced to operate with the zero voltage level (however, in this case, as shown in Fig. 2, the current path through the diodes is quite different). In this case, the voltage v_{ab} is 0 V. On the other hand, when the switching device *Sa* is off and the switching device *Sb* is on, the SP5L VIENNA rectifier is forced to operate with the voltage level $-v_{dc}/2$. Although the switching devices *Sa* and *Sb* are in the same state when compared with the positive half-cycle, as the SP5L VIENNA rectifier is operating in the negative half-cycle, the current path through the diodes is quite different: the voltage v_{ab} is $-v_{dc}/2$. When the switching device *Sa* is off and the switching device *Sb* is also off, the SP5L VIENNA rectifier is forced to operate with the voltage level v_{dc}: $-v_{dc}$. Also, depending on the voltage level, the inductance stores or delivers energy to the circuit.

III. MODEL-PREDICTIVE-CONTROL: DIGITAL IMPLEMENTATION

This section introduces the MPC based on fixed switching frequency applied to the SP5L VIENNA rectifier. It is imperative to mention that the SP5L VIENNA rectifier can also be controlled applying other current control strategies [20][21][22]. The main scope of this paper is the introduction of the MPC applied to control the grid-side current of the SP5L VIENNA rectifier, therefore, the details of the power theory are purposefully omitted, since it can be obtained by applying several algorithms with the objective to define the reference current. As example, when it is indispensable to obtain a sinusoidal reference for the grid-side current, it can be implemented the following equation:

$$i_i^*[n] = \frac{(v_{dc}[n]\, i_{dc}[n]) + p_c[n]}{V_{PLL}[n]\, V_{PLL}[n]}\, v_{pll}[n]\,, \tag{1}$$

where i_i* is the reference current, v_{dc} is the dc-link voltage, i_{dc} is the current on the dc-side, p_c is the power necessary to guarantee the controllability of the dc-link, V_{PLL} is the rms value of the grid-side voltage, obtained from a phase-locked loop (PLL), and v_{pll} is the instantaneous value of the grid-side voltage (from a PLL). Identifying the instantaneous value of the reference current, as well as the finite distinct states supported by the SP5L VIENNA rectifier, throughout every sampling period the MPC defines the variables that are compared with the PWM carrier to select the state of the SP5L VIENNA rectifier. Examining Fig. 1 on the grid-side, both in terms of voltages and currents, and applying the Kirchhoff law, it can be defined the relation:

$$\frac{di_i(t)}{dt} = \frac{v_i(t) - v_{ab}(t)}{L}, \tag{2}$$

where i_i is the current on the grid-side, v_i is the grid-side voltage, v_{ab} is the operating voltage of the SP5L VIENNA rectifier (which is constant during each sampling period, when assuming a constant dc-link voltage), and L is the inductance of the coupling filter. Utilizing the forward Euler process, results in:

$$\frac{i_i[n+1] - i_i[n]}{T} = \frac{v_i[n] - v_{ab}[n]}{L}. \tag{3}$$

Equation (3) defines the mathematical model used to control the SP5L VIENNA rectifier. Examining (3) is verified that the variables acquired in the instant $[n]$ are maintained with the same value during the respective sampling period, i.e., the variables acquired in $[n]$ are maintained with the same value during $[n, n+1]$. Since the objective is to apply an MPC, (3) can be rewritten in terms of the unknown variable, i.e., according to $i_i[n+1]$, such as:

$$i_i[n+1] = \frac{T}{L}(v_i[n] - v_{ab}[n]) + i_i[n]\,. \tag{4}$$

From the previous equations, knowing the reference current and the current measured in the instant [n], it is applied a cost function to minimize the error between both. In the scope of this paper, the cost function was selected with the clear objective to minimize the error according to:

$$J = \lambda \left(i_i^*[n+1] - i_i[n+1] \right), \quad (5)$$

where the weighting factor λ must be selected according to the parameters of the circuit, e.g., according to the value of the inductance (L) and the sampling frequency (f_s). With the established cost function, the weighting factor λ will define how precise the current control is, i.e., if the current i_i tracks its reference i_i* minimizing the error (the current ripple must be center-aligned with the reference to minimize the error). The reference current for [n+1] can be deduced based on [23]. The output of the cost function is then modified and compared with the unitary PWM carrier with the objective of defining the state of the SP5L VIENNA rectifier that pushes the current (i_i) to follow its reference (i_i*). Therefore, it is guaranteed the operation with a fixed switching frequency. The details of the PWM are presented in section IV.

IV. ANALYSIS AND VALIDATION

The validation of the MPC was conducted according to the conditions registered in Table I. The validation was performed with a fully developed model in PSIM software and considering real operating conditions.

TABLE I
PARAMETERS CONSIDERED IN THE PSIM SIMULATION MODEL

Parameter	VALUE
Grid-Side Voltage	230 V
Frequency (Grid-Side Voltage)	50 Hz
Dc-link Voltage	400 V
Maximum Power	4.6 kW
Coupling Filter	2 mH
Switching Frequency	20 kHz

Fig. 3 shows a steady-state result, where is presented the grid-side voltage (v_i), the current (i_i), as well as the operating voltage of the SP5L VIENNA rectifier (v_{ab}), defined according to the assumed state, where are clearly verified the five-levels established. In this figure, is shown that the grid-side voltage (v_i) and current (i_i) are sinusoidal, in addition, they are in phase, perfectly showing the operation as an active rectifier. Fig. 4 shows the same variables but considering that the grid-side voltage has harmonic content (THD value of 3.6%). This current is sinusoidal since the reference is also sinusoidal. It is also verified that the operating voltage of the SP5L VIENNA rectifier presents, as expected, five-levels. Such distortion of the voltage was obtained from real measurements in laboratory using a power quality analyzer (Fluke 435) with the objective of obtaining a simulation as reliable as possible. With the objective of analyzing, in more detail, the operation of the SP5L VIENNA rectifier in relation to the dc-link, Fig. 5 shows the current (i_i) on the grid-side, the operating voltage of the SP5L VIENNA rectifier (v_{ab}), and the currents in each source of the dc-link (i_{dc1} and i_{dc2}). This result was obtained to verify that it is possible to balance the voltages on the dc-link, and for that, it is possible to verify that the average value and the rms value of each of the currents (i_{dc1} and i_{dc2}) are equal, despite being symmetrical in relation to the half-cycle of the grid-side voltage (i.e., the i_{dc1} current in the positive half-cycle is equal to the i_{dc2} current in the negative half-cycle, and vice-versa). This result was obtained on steady-state and, as it can be seen, with the SP5L VIENNA rectifier operating with sinusoidal current.

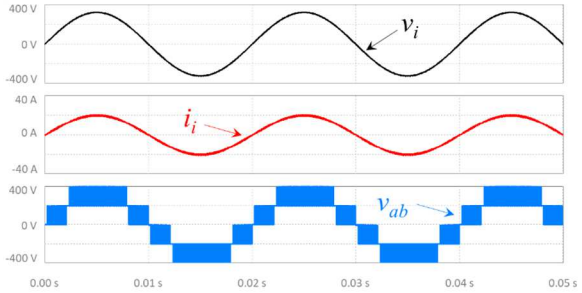

Fig. 3. SP5L VIENNA rectifier operating in steady-state with sinusoidal grid-side voltage and current: Grid-side voltage (v_i); Grid-side current (i_i); Voltage levels (v_{ab}).

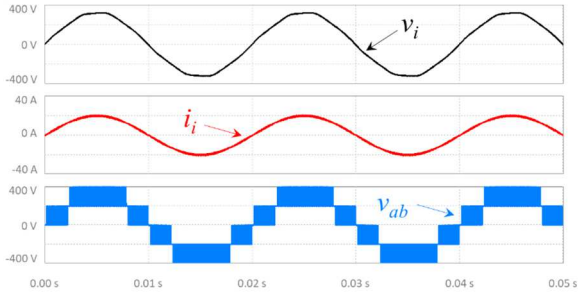

Fig. 4. SP5L VIENNA rectifier operating in steady-state with non-sinusoidal grid-side voltage and sinusoidal current: Grid-side voltage (v_i); Grid-side current (i_i); Voltage levels (v_{ab}).

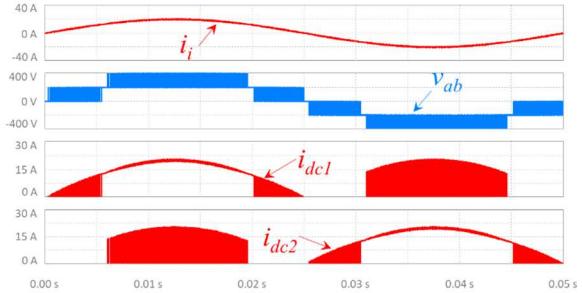

Fig. 5. SP5L VIENNA rectifier operating in steady-state: Grid-side current (i_i); Voltage levels (v_{ab}); Current on the split dc-link (i_{dc1}, i_{dc2}).

Fig. 6 shows the current (i_i) on the grid-side and the operating voltage of the SP5L VIENNA rectifier (v_{ab}). This result was obtained to verify the transition between voltage levels regarding the SP5L VIENNA rectifier voltages. Through this result, it is possible to verify that the ripple of the grid-side current (i_i) is smaller during the transition of voltage levels (in this specific case, when the transition occurs when the converter voltage no longer varies between 0 and $+v_{dc}/2$, but when changes between $+v_{dc}/2$ and $+v_{dc}$). The same situation happens when going through zero, where the ripple of the grid-side current is smaller. Fig. 7 also shows the current (i_i) on the grid-side and the operating voltage of the SP5L VIENNA rectifier (v_{ab}). This result allows to visualize the relationship between the current ripple and the operation state of the SP5L VIENNA rectifier, which defines its operating voltage. Analyzing in detail, it turns out that when it is operating with the voltage level $+v_{dc}/2$ it means that the inductance is storing energy, and when it is operating with the

voltage level $+v_{dc}$ it means that the inductance is supplying energy to the circuit.

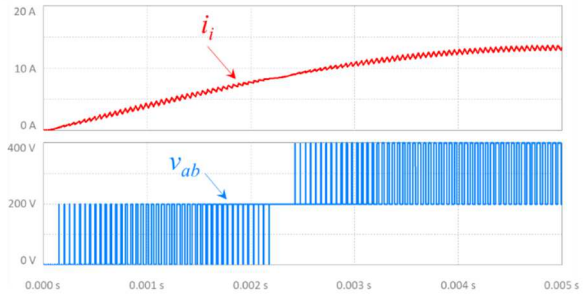

Fig. 6. SP5L VIENNA rectifier operating in steady-state showing in detail the grid-side current (i_i) and the transition from voltage levels (v_{ab}).

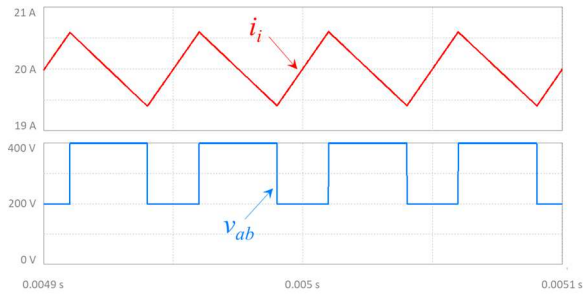

Fig. 7. SP5L VIENNA rectifier operating in steady-state showing in detail the grid-side current (i_i) and the voltage levels (v_{ab}) when vary between $+v_{dc}/2$ and $+v_{dc}$.

To verify the applicability of the MPC applied to the SP5L VIENNA rectifier, Fig. 8 shows the current (i_i) on the grid-side in comparison with its reference (i_i*). As it can be seen, the current follows its reference perfectly, maintaining a ripple with a fixed frequency, which is one of the main advantages of the proposed MPC applied to the SP5L VIENNA rectifier. Moreover, as it can be seen, the current i_i is properly centered on its reference i_i*, allowing to observe that, in this way, the error is zero. Fig. 9 shows the grid-side current (i_i) and the voltage applied to the IGBTs *Sa* and *Sb* (v_{Sa} and v_{Sb}). As it can be seen, the maximum voltage applied to each IGBTs is $v_{dc}/2$, representing an important characteristic of the SP5L VIENNA rectifier in comparison with traditional three-level solutions, where, for the same conditions, the maximum voltage is v_{dc}. Another important aspect that can be verified is that the IGBT *Sb* is only subjected to a maximum voltage of $v_{dc}/2$ when the operating voltage of the SP5L VIENNA rectifier varies between $+v_{dc}/2$ and $+v_{dc}$ (or between $-v_{dc}/2$ and $-v_{dc}$). On the contrary, the IGBT *Sa* is always subject to voltage variations (0 and $+v_{dc}/2$ or $+v_{dc}/2$ and $+v_{dc}$), regardless of the operating voltage of the SP5L VIENNA rectifier. In Fig. 10 it is possible to verify a current analysis also in the IGBTs *Sa* and *Sb*. As it can be seen, the current only circulates in the IGBT *Sa* when the voltage produced by the SP5L VIENNA rectifier varies between 0 and $+v_{dc}/2$, which is an interesting feature. On the other hand, the current in the IGBT *Sb* always circulates regardless of the operating voltage of the SP5L VIENNA rectifier. The maximum value of the current in each IGBT is, obviously, dependent on the current at the grid-side (in other words, it depends on the operating power of the SP5L VIENNA rectifier). As it turns out, the current always varies between 0 and a maximum value.

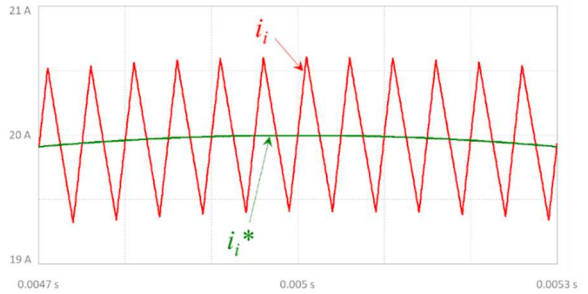

Fig. 8. SP5L VIENNA rectifier operating in steady-state showing in detail the comparison between the power grid current (i_i) and its reference (i_i*).

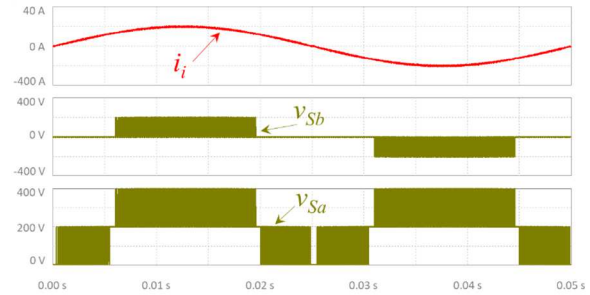

Fig. 9. SP5L VIENNA rectifier operating in steady-state showing the grid-side current (i_i) and voltage applied to the IGBTs *Sa* (v_{Sa}) and *Sb* (v_{Sb}).

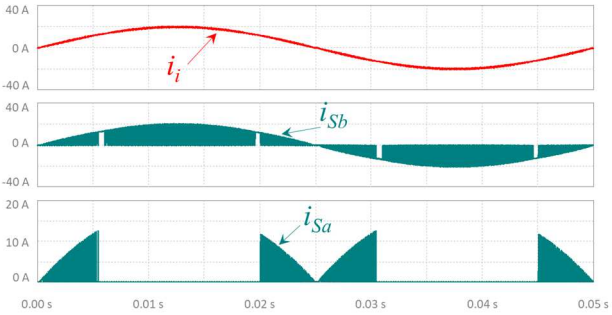

Fig. 10. SP5L VIENNA rectifier operating in steady-state showing the grid-side current (i_i) and current in the IGBTs *Sa* (i_{Sa}) and *Sb* (i_{Sb}).

Fig. 11 shows a detail of the current (i_i) on the grid-side and a detail of the currents in each IGBTs (i_{Sa} and i_{Sb}). The current i_i results from the direct sum of the currents i_{Sa} and i_{Sb}. In this specific case in which the converter is operating on the positive half-cycle, it is shown that when the current increases (the inductance stores energy), it flows through the IGBT *Sa* and when the current decreases (the inductance supplies energy) the current flows through the IGBT *Sb*. In this figure it is also verified that, obviously, the current never circulates through the two IGBTs at the same time. The time in which each of the IGBTs is on with respect to the switching period (duty-cycle) is defined by the control strategy to obtain a sinusoidal current. It is also important to verify that, obviously, whenever one IGBT is in the on state the other is in the off state. Fig. 12 shows the grid-side current (i_i), the reference current (i_i*), as well as the operating voltage (v_{ab}), with a sudden variation in the reference current. This variation was caused purposely to verify that the current i_i quickly follows its reference i_i* and that the voltage of the converter does not undergo sudden changes. Fig. 13 shows the same variables, where it is possible to verify the current i_i in detail and following its reference i_i* perfectly in about four control cycles (sampling time). As it can be seen, the variation of the reference current (i_i*) was 25%, both in the

first and second transition. When the first transition occurs, the SP5L VIENNA rectifier maintains the maximum voltage level (i.e., $+v_{dc}$) so that the current i_i reaches its reference as quickly as possible (in this case the current must decrease). When the second transition occurs, the converter maintains the voltage level $+v_{dc}/2$, also so that the current i_i reaches its reference as quickly as possible (in this case the current must increase). The most important thing to highlight from this result is that it is verified that the current is always centralized in its reference.

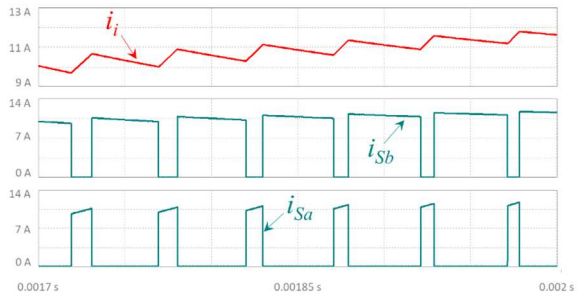

Fig. 11. SP5L VIENNA rectifier operating in steady-state showing in detail the grid-side current (i_i) and current in the IGBTs *Sa* (i_{Sa}) and *Sb* (i_{Sb}).

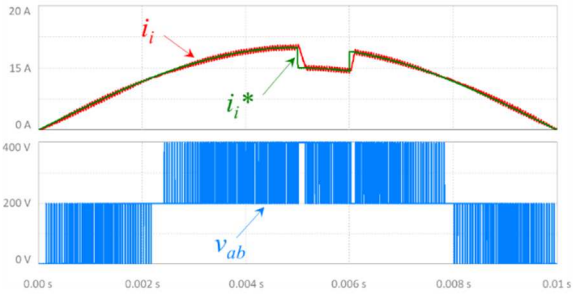

Fig. 12. SP5L VIENNA rectifier operating in transient-state showing the comparison between the grid-side current (i_i) and its reference (i_i*), as well as the operating voltage levels (v_{ab}).

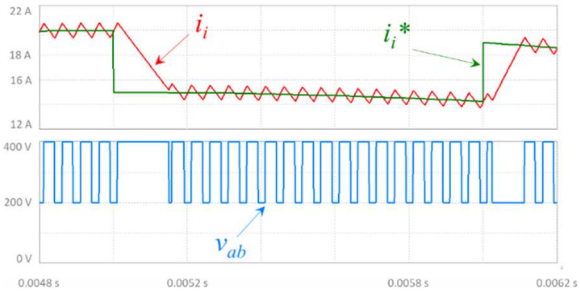

Fig. 13. SP5L VIENNA rectifier operating in transient-state showing in detail the comparison between the grid-side current (i_i) and its reference (i_i*), as well as the operating voltage levels (v_{ab}) when vary between $+v_{dc}/2$ and $+v_{dc}$.

Fig. 14 shows a case to verify the applicability of the MPC applied to the SP5L VIENNA rectifier, showing the voltage (v_i), the current (i_i) and the operating voltage (v_{ab}). It is verified that the voltage presents harmonic distortion to obtain real operating conditions. However, it was considered a non-sinusoidal reference current, but triangular, whose fundamental frequency is equal to the fundamental frequency of the grid-side voltage. As previously mentioned, this is an extreme case in which it is only intended to verify the applicability of the MPC and, as it can be seen, the current has a triangular waveform and the SP5L VIENNA rectifier continues to operate with the five voltage levels. Regarding the implemented PWM strategy, Fig. 15 shows the PWM carrier (c_{pwm}), the comparison signals with the PWM carrier (a_{pwm} and b_{pwm}), as well as the gate-emitter voltages applied to the IGBTs *Sa* and *Sb* (v_{gsSa} and v_{gsSb}). A strategy with a modified sinusoid (for the a_{pwm} signal) is used to compare with the PWM carrier (c_{pwm}) in order to obtain the control signals for the IGBT *Sb* and the b_{pwm} signal is used to compare with the PWM carrier (c_{pwm}) to obtain the control signals for the IGBT *Sa*.

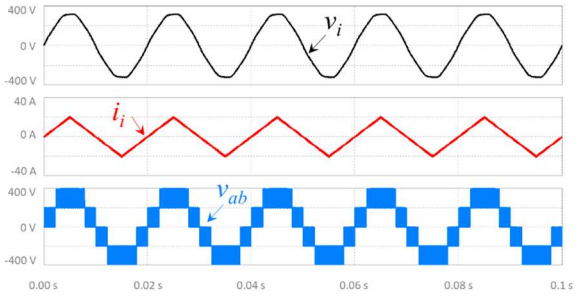

Fig. 14. SP5L VIENNA rectifier operating in steady-state with non-sinusoidal grid-side voltage and non-sinusoidal current to verify the precise application of the MPC: Grid-side voltage (v_i); Grid-side current (i_i); Voltage levels (v_{ab}).

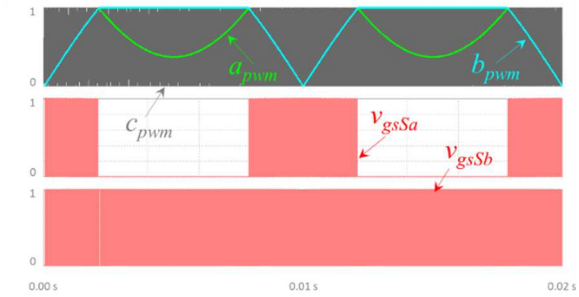

Fig. 15. Detail of the PWM applied to the SP5L VIENNA rectifier showing the carrier (c_{pwm}), the control signals (a_{pwm} and b_{pwm}), and the gate-emitter voltages applied to the IGBTs (v_{gsSa} and v_{gsSb}).

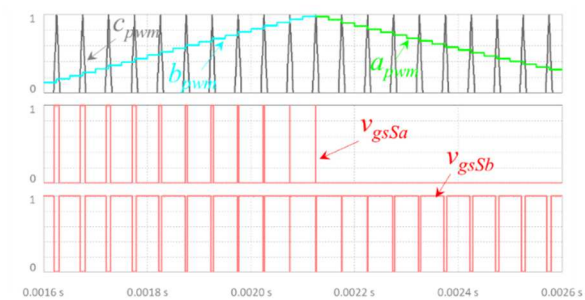

Fig. 16. Detail of the PWM applied to the SP5L VIENNA rectifier showing in detail the carrier (c_{pwm}), the control signals (a_{pwm} and b_{pwm}), and the gate-emitter voltages applied to the IGBTs (v_{gsSa} and v_{gsSb}).

The same signals are shown in Fig. 16, but in more detail. As it turns out, this detail was purposely obtained to verify the moment of transition. For the case of IGBT *Sa*, it is verified that it remains in the on state when the carrier is higher than the b_{pwm} signal, and the inverse is verified in relation to the IGBT *Sb* and the respective comparison signal with the PWM carrier. Even in more detail in relation to the previous figures, the same variables are shown in Fig. 17, but allowing to interpret the operating principle of the proposed PWM more easily. It is shown that the signals b_{pwm} and a_{pwm} are the same (this situation only occurs when the converter voltage varies between 0 and $+v_{dc}/2$ or between 0 and $-v_{dc}/2$).

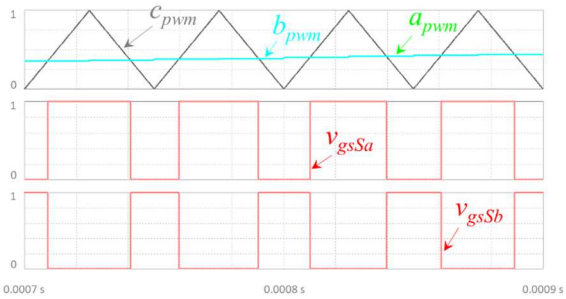

Fig. 17. Detail of the PWM applied to the SP5L VIENNA rectifier showing the carrier (c_{pwm}), the control signals (a_{pwm} and b_{pwm}), and the gate-emitter voltages applied to the IGBTs (v_{gsSa} and v_{gsSb}).

V. CONCLUSIONS

A single-phase five-level (SP5L) VIENNA rectifier is introduced, where the control is determined by a model-predictive-control (MPC). The paper covers these two important aspects: the principle of operation and differencing advantages of the SP5L VIENNA rectifier compared with the traditional active rectifiers; and the MPC, which presents as main contribution the possibility to control the grid-side current with fixed switching frequency. The main advantages of the SP5L VIENNA rectifier are highlighted, including an analysis concerning the voltage levels, the voltage applied to each semiconductor, and the circulating current. The validation was performed for steady-state and transient-state, as well as for considering different waveforms for the reference current, where the results show the precise application of the MPC. In the obtained results it is clearly verified that the five-levels are established, independently of the reference current and the harmonic distortion of the grid-side voltage, and that it is possible to balance the split dc-link. In terms of current, it was observed that the current follows its reference, properly centered to minimize the error, and maintaining a ripple with a fixed frequency, which is one of the main advantages of the applied MPC. Concluding, it was proved the accurate and precise application of a MPC, based on fixed switching frequency, applied to the SP5L VIENNA rectifier.

ACKNOWLEDGMENT

This work has been supported by FCT – Fundação para a Ciência e Tecnologia within the R&D Units Project Scope: UIDB/00319/2020. This work has been supported by the FCT Project newERA4GRIDs PTDC/EEI-EEE/30283/2017, and by the FCT Project DAIPESEV PTDC/EEI-EEE/30382/2017. Tiago Sousa is supported by the doctoral scholarship SFRH/BD/134353/2017 granted by FCT.

REFERENCES

[1] Vítor Monteiro, B. Exposto, J. Ferreira, João L. Afonso, "Improved Vehicle-to-Home (iV2H) Operation Mode: Experimental Analysis of the Electric Vehicle as Off-Line UPS," IEEE Transactions on Smart Grid, vol.8, no.6, pp.2702-2711, Nov. 2017.

[2] E. Barbie, R. Rabinovici, A. Kuperman, "Modeling and Simulation of a Novel Active Three-Phase Multilevel Power Factor Correction Front End – The "Negev" Rectifier," IEEE Trans. Energy Conversion, vol.35, no.1, pp.462-473, Mar. 2020.

[3] J. Benzaquen, B. Mirafzal, "Seamless Dynamics for Wild-Frequency Active Rectifiers in More Electric Aircraft," IEEE Trans. Ind. Electron., vol.67, no.9, pp.7135-7145, Sept. 2020.

[4] Vitor Monteiro, J. Ferreira, A. Melendez, Carlos Couto, João L. Afonso, "Experimental Validation of a Novel Architecture Based on a Dual-Stage Converter for Off-Board Fast Battery Chargers of Electric Vehicles," IEEE Trans. Veh. Tech., vol.67, no.2, pp.1000-1011, Feb. 2018.

[5] Bhim Singh, Brij N. Singh, Ambrish Chandra, Kamal Al-Haddad, Ashish Pandey, Dwarka P. Kothari, "A Review of Single-Phase Improved Power Quality AC-DC Converters," IEEE Trans. Ind. Electron., vol.50, no.5, pp.962-981, Oct. 2003.

[6] Q. Huang, A. Q. Huang, "Hybrid Low-Frequency Switch for Bridgeless PFC," IEEE Trans. Power Electron., vol.35, no.10, pp.9982-9986, Oct. 2020.

[7] M. Rivera, D. Faundez, S. Toledo and J. Kolar, "A Review of AC-DC Converters with Injection Circuits - Part I," 2018 IEEE International Conference on Automation/XXIII Congress of the Chilean Association of Automatic Control (ICA-ACCA), 2018.

[8] M. Rivera, D. Faundez, S. Toledo and J. Kolar, "A Review of AC-DC Converters with Injection Circuits - Part II," 2018 IEEE International Conference on Automation/XXIII Congress of the Chilean Association of Automatic Control (ICA-ACCA), pp.1-5, 2018.

[9] Johann W. Kolar, Thomas Friedli, "The Essence of Three-Phase PFC Rectifier Systems—Part I," IEEE Trans. Power Electron., vol.28, no.1, pp.176-198, Jan. 2013.

[10] Thomas Friedli, Michael Hartmann, Johann W. Kolar, "The Essence of Three-Phase PFC Rectifier Systems—Part II," IEEE Trans. Power Electron., vol.29, no.2, pp.543-560, Feb. 2014.

[11] F. Musavi, M. Edington, W. Eberle, W. Dunford, "Evaluation and Efficiency Comparison of Front-End AC-DC Plug-in Hybrid Charger Topologies," IEEE Trans. Smart Grid, vol.3, pp.413-421, Mar. 2012.

[12] W. Zhu, C. Chen, S. Duan, T. Wang, P. Liu, "A Carrier-Based Discontinuous PWM Method With Varying Clamped Area for Vienna Rectifier," IEEE Trans. Ind. Electron., vol.66, no.9, pp.7177-7188, Sept. 2019.

[13] T. Wang, C. Chen, P. Liu, W. Zhu, S. Duan, "A Current Control Method With Extended Bandwidth for Vienna Rectifier Considering Wide Inductance Variation," IEEE Journal of Emerging and Selected Topics in Power Electronics, vol.9, no.1, pp.590-601, Feb. 2021.

[14] T. Wang, C. Chen, P. Liu, T. Liu, Z. Chao, S. Duan, "A Hybrid Space-Vector Modulation Method for Harmonics and Current Ripple Reduction of Interleaved Vienna Rectifier," IEEE Trans. Ind. Electron., vol.67, no.10, pp.8088-8099, Oct. 2020.

[15] L. Zhang et al., "A Modified DPWM With Neutral Point Voltage Balance Capability for Three-Phase Vienna Rectifiers," IEEE Trans. Power Electron., vol.36, no.1, pp.263-273, Jan. 2021.

[16] J. Gao, C. Gong, W. Li, J. Liu, "Novel Compensation Strategy for Calculation Delay of Finite Control Set Model Predictive Current Control in PMSM," IEEE Trans. Ind. Electron., vol.67, no.7, pp.5816-5819, July 2020.

[17] R. Guzman, L. Vicuña, A. Camacho, J. Miret, J. Rey, "Receding-Horizon Model-Predictive Control for a Three-Phase VSI With an LCL Filter," IEEE Trans. Ind. Electron., vol.66, pp.6671-6680, Sept. 2019.

[18] S. Liu, C. Liu, "Virtual-Vector-Based Robust Predictive Current Control for Dual Three-Phase PMSM," IEEE Trans. Ind. Electron., vol.68, no.3, pp.2048-2058, Mar. 2021.

[19] Vítor Monteiro, A. Meléndez, J. Ferreira, C. Couto, João L. Afonso, "Experimental Validation of a Proposed Single-Phase Five-Level Active Rectifier Operating with Model Predictive Current Control," IEEE IECON Ind. Electronics Conference, pp.3939-3944, Nov. 2015.

[20] Vítor Monteiro, T. Sousa, J. Martins, M. Sepúlveda, C. Couto, João L. Afonso, "Sliding Mode Control of an Innovative Single-Switch Three-Level Active Rectifier," IEEE SEST International Conference on Smart Energy Systems and Technologies, Porto, Portugal, pp.1-6, Sept.2019.

[21] Vítor Monteiro, A. Meléndez, C. Couto, João L. Afonso, "Model Predictive Current Control of a Proposed Single-Switch Three-Level Active Rectifier Applied to EV Battery Chargers," IEEE IECON Ind. Electronics Conference, Florence Italy, pp.1365-1370, Oct. 2016.

[22] André F. López, V. M. López-Martín, F. J. Azcondo, L. Corradini, A. Pigazo, "Current-Sensorless Power Factor Correction With Predictive Controllers," IEEE Journal of Emerging and Selected Topics in Power Electronics, vol.7, no.2, pp.891-900, June 2019.

[23] A. Sabanovic, K. Jezernik, N. Sabanovic, "Sliding Modes Applications in Power Electronics and Electrical Drives," Springer Variable Structure Systems: Towards the 21st Century, pp.223-251, 2002.